Tone Mapping and Blending Method to Improve SAR Image Visibility

Satoshi Hisanaga, Koji Wakimoto and Koji Okamura

Abstract—It is possible to interpret the shape of buildings based on synthetic aperture radar (SAR) images acquired using airborne SAR systems. However, the pixel values of SAR images have a high dynamic range intensity, and SAR images cannot be displayed without dynamic range intensity compression. Thus, we have developed a tone mapping method and a blending method. Using our method, the tone of SAR images becomes seamless with no intensity gap.

Index Terms—synthetic aperture radar, visualization, dynamic range intensity compression.

I. INTRODUCTION

SAR images are used to observe the shape of ground structures during damage assessment after a disaster. The intensities of backscattered microwave pulses are reflected from the ground and expressed in SAR images as pixel values. Pixel values are lower over flat ground. However, pixel values increase in some cases due to backscattering from metal objects. This indicates that the pixel values have a high dynamic range. The conventional method used to display SAR images contains a drawback: without compression of intensity with dynamic range, SAR images cannot be displayed with adequate contrast. Furthermore, the pixel values of SAR images contain speckle noise. This means that the intensity of SAR images partially changes at random. Although studies have looked into both multi look methods and backscattering estimation methods as a means to address this issue, there seems to be no established method to erase speckle noise[1], [2].

Thus, we treated an SAR image as a high dynamic range image (HDRI) and conducted studies to improve the visibility of an HDRI. A previous study on an HDRI display system was conducted by Seetzen[3]. The study also investigated the distinctive threshold of the human visual system. It was found that 1,200 is the maximum number of distinguishable steps in brightness that humans can perceive on a display[4], [5]. This restriction implies that the dynamic range of intensity has to be compressed to within 1,200 steps, while at the same time maintaining a sufficient difference in intensity that allows artificial objects to remain interpretable. Lambers et al. applied several intensity compression methods designed for optical images toward the evaluation of SAR images[6]. Their evaluation results demonstrated the need to develop methods tailored to multiplicative speckle and the presence of

high peaks with small spatial extensions. An edge-preserving filter has also been investigated for use in displaying images with high dynamic range intensity[7]. However, the edge-preserving filter smoothes out areas without edges, and it is therefore not suitable for SAR images in which the edges are not clear. We had developed the method adopts a different compression level for each area[8]. However, the method has the drawback that gaps occur in the border areas with different tone mapping. We developed a blending method capable of displaying seamless SAR images without intensity gaps.

II. SAR IMAGE

Fig. 1 shows an example of a SAR image. The left side of the figure is an aerial photograph taken by the Geographical Survey Institute of Japan in 2007. The right side of the figure is a graph illustrating the pixel values of the SAR image in the z axis. According to the aerial photograph, the upper
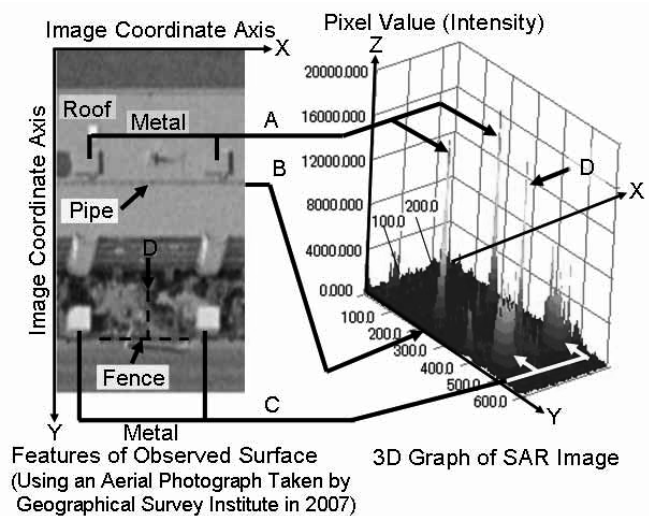

Fig. 1. Example of SAR Image

part of this SAR image seems to show the flat roof of a building. Additionally, there are four square metal regions and a metal pipe on the roof. One-third of the SAR image seems to show plants on the ground. There are also two sections containing metal materials. Arrows A and C in Fig. 1 show the intensities of these metal materials. Fig. 1 shows the intensity graph of the square region, which is expressed as a mountainous shape with a high peak in the SAR image. The arrow D in Fig. 1 shows the intensity of a metal fence. The intensity is not flat along the fence. In addition, there are a few differences in the intensity of the pipe (arrow B in Fig. 1) and the flat roof.

We applied gamma intensity compression, equalized intensity compression, and a bilateral filter to the HDRI example

Fig. 2. Intensity Compression Results by General Methods
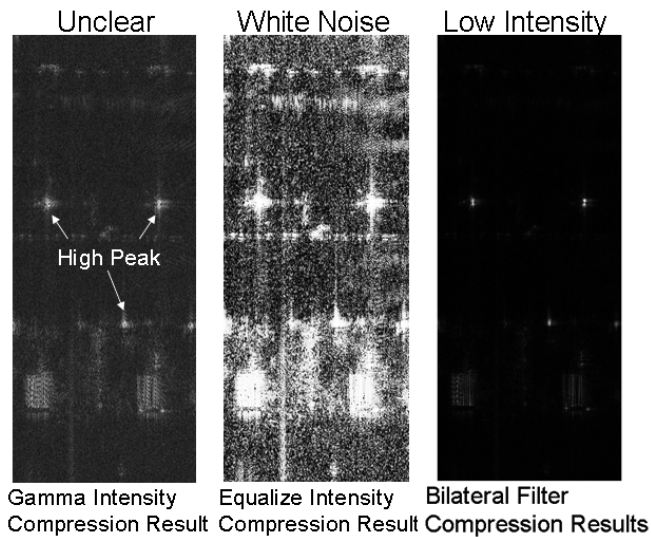
Fig. 3. Fllow of Intensity Compression Method

Fig. 4. Region Growing Method

of intensity compression.

Fig. 2 shows the results of dynamic range intensity compression using general methods. In Fig. 2, the left image is the result of using the gamma compression method. These images are unclear. The results obtained using the gamma compression method are unclear because of a high peak, while arrow A in Fig. 1 and high peaks in Fig. 2 are also not clearly displayed. The middle figure is the result of using the histogram equalization method. In Fig. 2, the square objects can be interpreted using the results obtained from the histogram equalized compression method. However, other objects cannot be distinguished from image noise. The right figure, which shows the result of using the bilateral filter, is also unclear, although the square objects can be distinguished. However, other objects have low intensity.

III. INTENSITY COMPRESSION METHOD

We focused on the fact that large changes in pixel values occur around regions containing artificial materials. However, the pixel values representing artificial materials are not similar to speckles and high peaks. Thus, we used an approach for clustering the changing pixel values by area with the purpose of detecting areas containing artificial materials. We also applied an intensity compression method at different levels in each area. The system also blends the intensity of clusters to display SAR images without a difference-of-intensity gap (See Fig. 3). We begin by describing the clustering method and the compression method we developed d[8]. We then describe the blending method.

A. Clustering Method

The problems inherent in the use of clustering for SAR images are as follows.

- Speckle noise appears on SAR images.
- High peak noise appears on SAR images.
- The intensity of artificial objects is uncertain.

Based on these problems, there is a difference in the intensities of artificial objects and neighborhoods without a clear edge. Because the intensities of artificial objects are
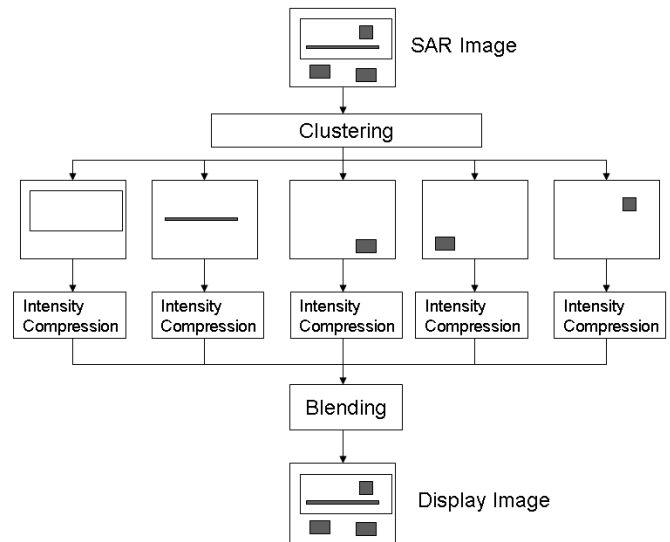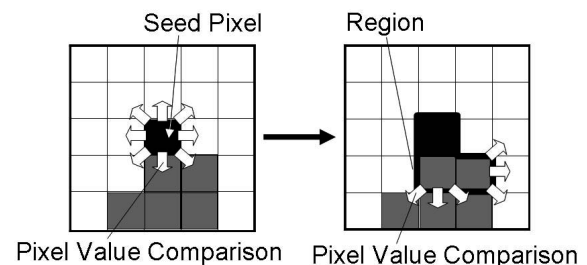
unclear, applying a clustering method using a threshold level is not suitable.

We adopted an approach to cluster pixels together that show little difference in their intensities. Fig. 4 shows a region growing method. Using this method, the system clusters artificial objects within an area.

Fig. 5 shows the clustering method. First, in order to reduce a small gap in the pixel values, the system processes summit levels operating in an SAR image. Formula 1 illustrates this summit levels operation. In formula, I is the intensity, and N is the neighborhood. The summit level operation replaces the small gap in pixel values with the maximum intensity of the neighborhood. Fig. 6 shows an example of the summit level operation. The left section of Fig. 6 is a SAR image. In the image, there are gaps in the intensity of the pixel values because the pixels alternately take large and small values. The right section of Fig. 6 shows the results of a summit level operation in which there are no gaps in intensity in order to prevent the occurrence of clustering.

$$I(X,Y) = Max\{I(X',Y')|(X',Y') \in N(X,Y)\} \quad (1)$$

Next, the system operates a Laplacian filter for the image in order to detect large changes in pixel value. To choose the position of an artificial material on a SAR image, the system clusters gather into areas with high pixel values due to Laplacian processing and k-means clustering[9]. The k-means method is used due to its effectiveness in clustering discrete points. The system determines the area of an artificial
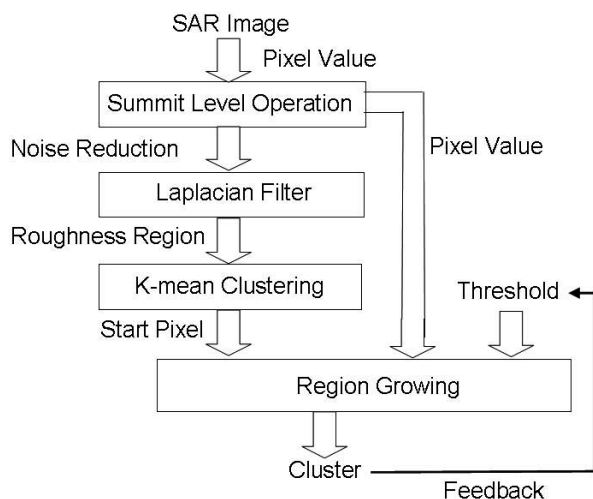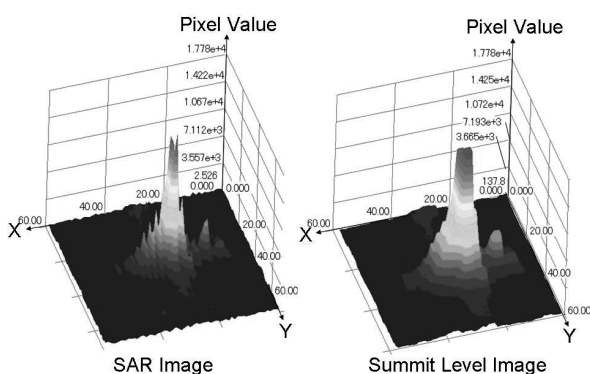
Fig. 5.   Clustering Method

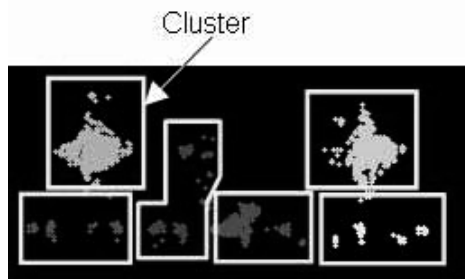Fig. 6.   SAR Image and Summit Level Image

Fig. 7.   Laplacian Filter and k-means Clustering Result

Fig. 8.   Relationship Between the Number of Pixels and Threshold

Fig. 9.   Region Growing Results

Fig. 10.   Histogram of Region

material on a SAR image using the region growing method (See Fig. 7).

Since the operation for stopping a growing region at a threshold of intensity is not fixed, we attempted to fix the threshold of intensity using the number of the pixels in the cluster. Fig. 8 shows the relationship between the number of pixels in a cluster and the threshold of intensity. The number of pixels in a cluster increases with a decrease in the threshold level. We considered that an increase of pixels in a cluster results from a connection of areas with artificial metal with other areas. In Fig. 8, the area with artificial metal is fixed using threshold B. For threshold A, the number of pixels is not sufficient. On the contrary, for threshold C, the cluster includes unnecessary pixels (See Fig. 9).
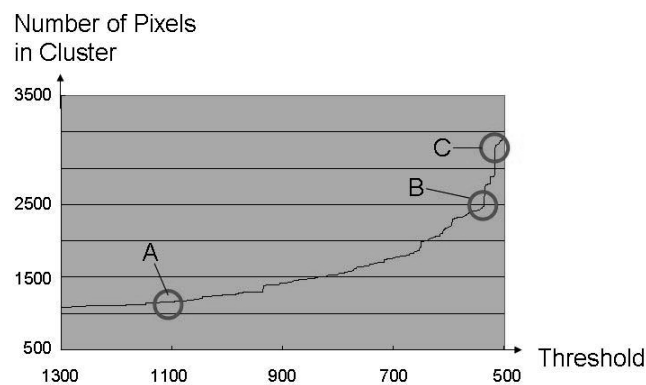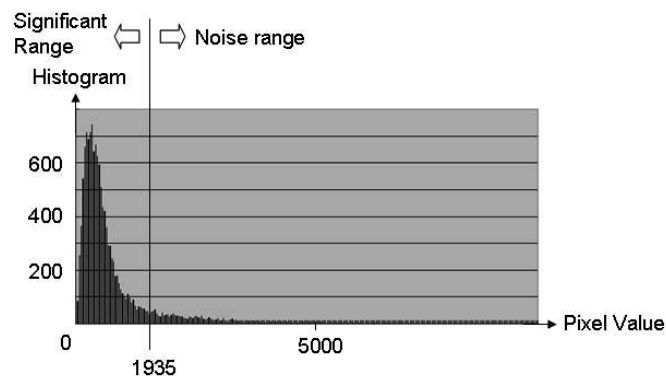
B. Intensity Compression Method

For a SAR image, the general intensity compression method for electro-optical images is not suitable. We used two approaches for SAR image intensity compression.

The first approach is a histogram equalization method for increasing contrast. The second approach uses both an estimation method for image noise levels and a linear intensity compression method. In this way, we assume image noise as a small region with high peak intensity. Because, it is assumed that the number of higher intensity pixels which belong to noise is less than the number of high intensity pixels which belong to metal objects. The detection rate of the metal object can be improved by this assumption, though the possibility of underdetecting the noise increases. Fig. 10 shows a histogram of the artificial metal area shown in Fig. 9. The system determines a pixel value as the threshold of

noise, where the incline of the histogram for the pixel level becomes more than the determined value. In the example shown in Fig. 10, the threshold becomes 1,935 pixels. The system compresses the intensity in the area of the artificial metal using the equalization method with an intensity of less than 1,935 pixels.

Fig. 11 shows the effects of using a low-pass filter. Differences in intensity less than the threshold become visible. Fig. 12 shows the results of intensity compression. The left-side of Fig. 12 shows the results of histogram equalization in an entire image for comparison. The center of the image is the result of histogram equalization in an artificial metal area. The right image in the figure shows the results of intensity-limited linear equalization. Histogram equalization results in noise throughout the entire image. Both the results from histogram equalization and intensity-limited linear equalization are clearer than the results achieved using histogram equalization. Moreover, the results from intensity-limited linear equalization are the clearest.
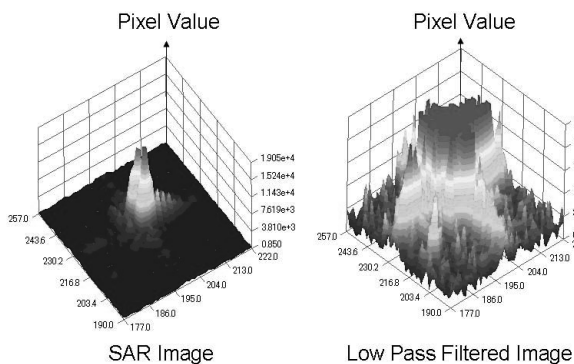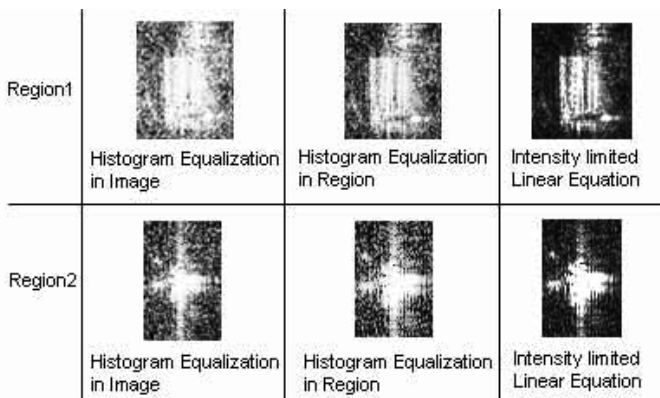

Fig. 11.   Effect of Low Pass Filter

Fig. 12.   Intensity Compression Results

C. Blending Method

The intensity gap at the border of clusters that are separately compressed is very prominent because the range of intensity is different (Fig.13). We focused on the Alfa blending method, which is used to synthesize images. However, it is aimed at synthesizing different images. In our method, the same image was the object of the synthesis, although the range of intensity was different. We assumed that the method to synthesize the pixel values was linear, but the method of conversion gradually increased the range of intensity. Fig.14

shows the conversion result. The right of the figure shows the range, which was transformed by our method. The border of different ranges was smoothed. As a result, the gap between the areas became seamless, as shown in the left of the figure.
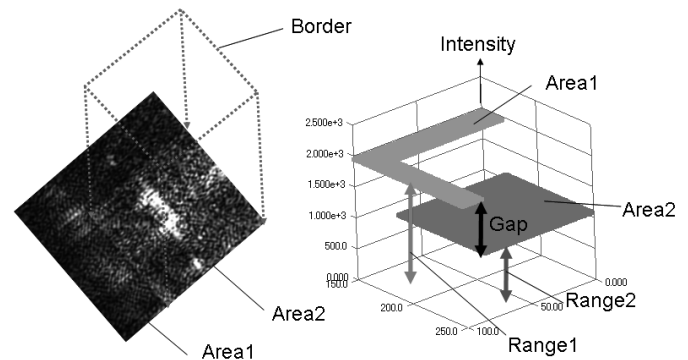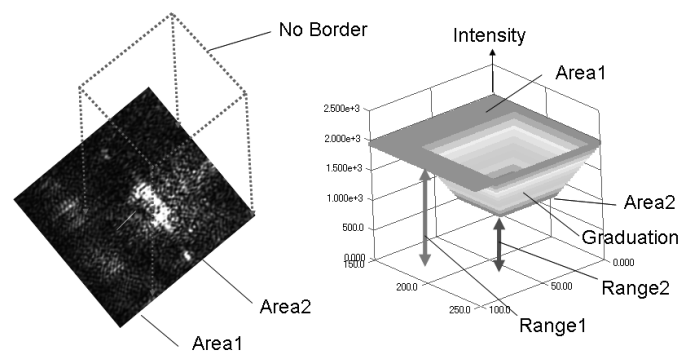

Fig. 13.   Example of Intensity Gap

Fig. 14.   Range Conversion

IV. EXPERIMENT RESULT

The tone mapping result is shown first. The images on the left of Fig. 15 show the area where the artificial material is detected.

The experimental results are as follows: of the eleven artificial material clusters detected on the SAR image, two clusters ((a6) and (b1) in Fig. 15) were larger than the artificial materials, while one cluster ((c) in Fig. 15) was smaller. The area a6 in Fig. 15 became large because the region-growing method did not end due to small differences in intensity around the objects. With cluster b1, the minimum bounding rectangle became large because both the height and width of the area were high. In contrast, cluster c had a high peak pixel as the starting pixel of the region of growth; therefore, c stopped at the high pixel value. A small region containing artificial material was not detected ((d1), (d2), and (d3) in Fig. 15) because the areas of high intensity were small and well separated in location.

The right figure shows the results of high dynamic range intensity compression. The edges of the artificial material are displayed more clearly than in the case in which the intensity compression image (shown in Fig. 2) is obtained using general methods.

For clusters a1-a6 in Fig. 15, the amount of noise decreased and the contrast increased. In particular, the edge of the artificial metal objects became clearer around a4 and a6.
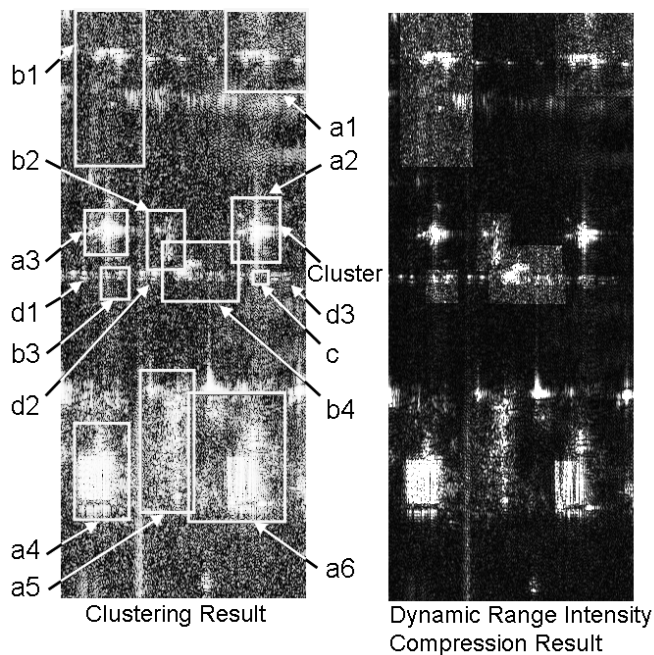
Fig. 15.   Tone Mapping Result by Our Method

Fig. 17.   Range Gap of Tone Mapping Result

For clusters a1, a2, a3, and a5, the edges of the artificial metal objects were not very clear due to noise on the SAR image. However, the location of the metal objects became clearer as the intensity of the area without metal objects was reduced. The noise decreased with clusters b1-b4. However, the contrast did not increase sufficiently. Thus, at a low contrast, the intensity of the metal objects did not have a high value compared with the neighboring areas around b1-b4. The system compressed the intensity of the area without detecting artificial metal using linear method.

Fig. 16 shows the pixel value of the area where the metal was not detected. At the center of the image, there is an area where a high peak is seen. This pixel has the possibility of indicating metal. Other pixels did not have a high value. During tone mapping, the noise level was estimated from the histogram for this area.
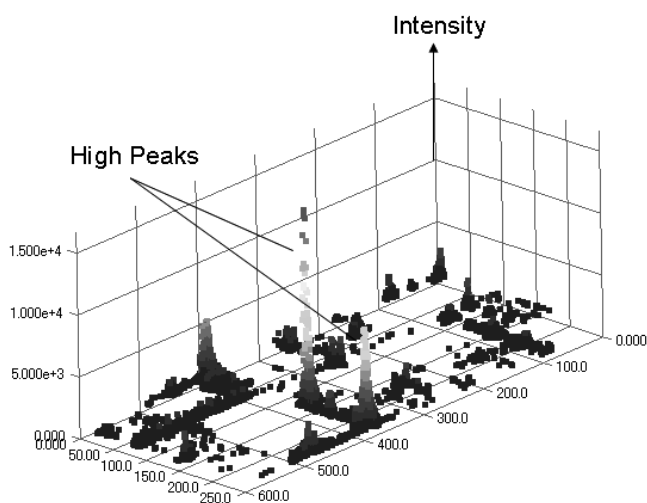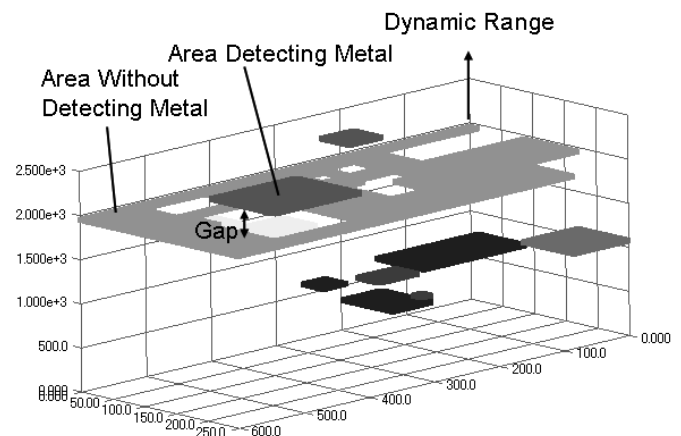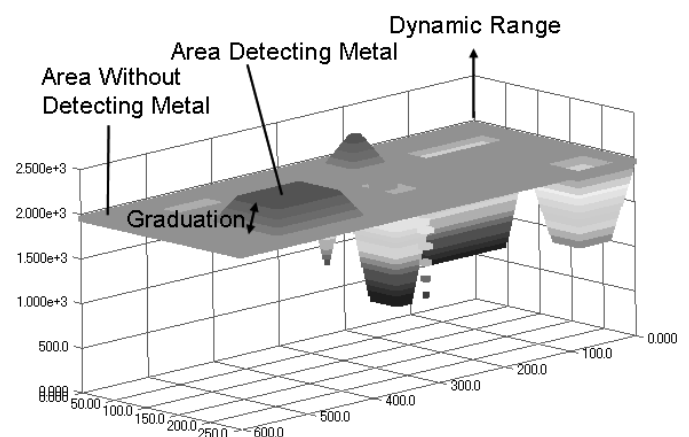

Fig. 18.   Range Conversion Result by Our Method

The blending result is shown next. Fig. 17 shows differences of the dynamic range in the tone mapping results. The largest area did not require tone mapping. The largest area was assumed to be a standard range. The range of some areas was wider than that of the standard, while the range of other areas was narrower than that of the standard. The range was converted by our method, as shown in Fig. 18. This indicates that the range difference in the borders of the area was gradually changed. Intensity gap on the right of Fig. 19 is less than that on the left of the figure.

V. Conclusion

We developed a dynamic range intensity compression method suitable for SAR image features. The main feature of our method is that the system applies a different level compression ratio to each area. The visibility of SAR images was improved using our method. However, there was a problem of under-detection using the clustering method. The gap does not disappear completely because the shape of the area does not correspond to the metal shape. In future work, more research is required on the clustering of artificial metal objects in SAR images to further improve visibility.
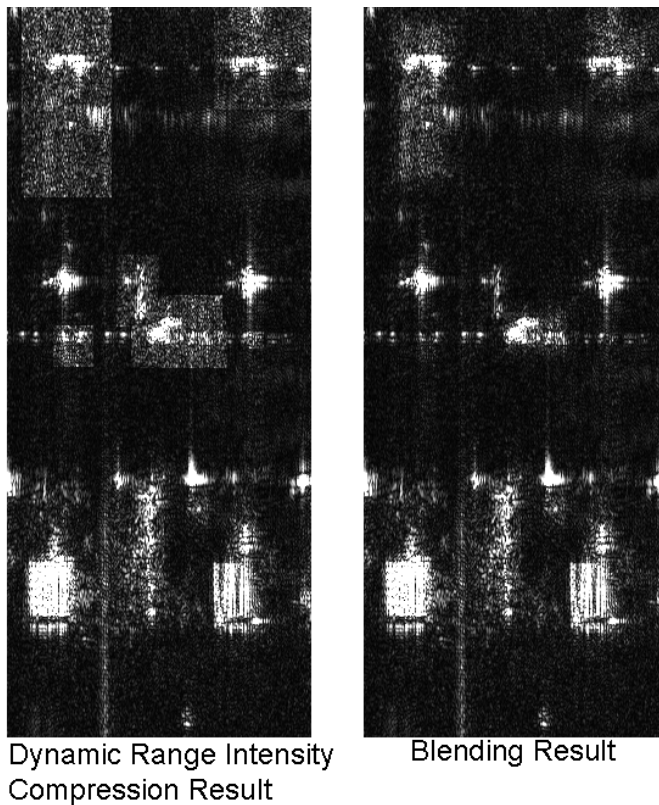

Fig. 16.   Intensity of Area Without Metal

Fig. 19. Tone Mapping and Blending Result

REFERENCES

[1] M.R. Azimi-Sadjadi and S. Bannour, Two-dimensional adaptive block Kalman filtering of SAR imagery, IEEE Transactions on Geoscience and Remote Sensing, vol. 29, pp. 742-753, 1991

[2] J. S. Lee, Digital image enhancement and noise filtering by use of local statistics, Pattern Analysis and Machine Intelligence, vol. PAMI-2, pp. 165-168, 1980

[3] H. Seetzen, W. Heidrich, W. Stuerzlinger, G. Ward, L. Whitehead, M. Trentacoste, A. Ghosh, A. Vorozcovs, High Dynamic Range Display Systems, Proc. ACM SIGGRAPH 2004, pp. 760-768, 2004

[4] Peter G. J. Barten, Physical model for the contrast sensitivity of the human eye, Proc. SPIE Human Vision, Visual Processing, and Digital Display III, vol. 1666, pp. 57-72, 1992

[5] Peter G. J. Barten, Spatio-temporal model for the contrast sensitivity of the human eye and its temporal aspects, Proc. SPIE Human Vision, Visual Processing, and Digital Display IV, vol. 1913, pp. 2-14, 1993

[6] M. Lambers, H. Nies, A. Kolb, Interactive Dynamic Range Reduction for SAR Images, Geoscience and Remote Sensing Letters, Vol. 5 Issue3 pp. 507-511, 2008

[7] Fredo Durand, Julie Dorsey, Fast bilateral filtering for the display of high-dynamic-range images, ACM Transactions on Graphics (TOG), Vol. 21 Issue 3 , pp. 844-847, July 2002

[8] S. Hisanaga, K. Wakimoto, K. Okamura, Compression Method for High Dynamic Range, Lecture Notes in Engineering and Computer Science: Proceedings of The International MultiConference of Engineers and Computer Scientists 2011, IMECS 2011, 16-18 March, 2011, Hong Kong, pp589-593

[9] J. MacQueen, Some methods for classification and analysis of multivariate observations, Proc. the Fifth Berkeley Symposium on Mathematical Statistics and Probability, Vol. I, Statistics, L. M. Le Cam and J. Neyman (Eds.) , University of California Press, pp. 281-297, 1967

[10] T. Tasdizen and R. Whitaker, Feature preserving variational smoothing of terrain data, IEEE Transactions on Geoscience and Remote Sensing, Issue Date: Oct. 2006 Vol. 44 Issue 10 pp. 2983 - 2990, 2006